Inclusion and release of ant alarm pheromones from metal-organic frameworks

Harina Amer Hamzah, Daniel Rixson, Joseph Paul-Taylor, Huan V. Doan, Christopher Dadswell, Gavin Roffe, Arun Sridhar, Claire L. Hobday, Charlie Wedd, Tina Düren, William O. H. Hughes, John Spencer and Andrew D. Burrows

Electronic supplementary information

1. General experimental details

All reagents and solvents were purchased from commercial sources and used without further purification.

Powder X-ray diffraction (PXRD) patterns for all samples were recorded on a Bruker AXS D8 Advance diffractometer with copper K_α radiation (λ = 1.5406 Å) at 298 K. The beam slit was set to 1 mm, detector slit set to 0.2 mm and anti-scattering slit set to 1 mm. Samples were dried in ambient conditions and ground using a pestle and mortar. The powders were packed onto a flat plate and measured with a 2θ range of 5 – 60°. The step size was 0.024° with the scan speed set to 0.3 s per step.

^{1}H NMR spectra were recorded on the digested MOFs at 298 K on a Bruker Avance 300 MHz Ultrashield spectrometer or an Agilent 500 MHz ProPulse spectrometer. All ^{1}H NMR spectra were referenced to the residual *protio* peaks at δ 2.50 ppm for DMSO-d_6. For the UiO-66 materials, a typical MOF digestion was carried out by adding 10 mg of a crystalline sample into 0.4 mL of DMSO-d_6 and 0.2 mL of a stock solution of NH_4F in D_2O (4.14 M). For the IRMOF materials, the MOF digestions were each carried out using approximately 10 mg of crystalline sample in 0.4 mL of DMSO-d_6 and 0.2 mL of a stock solution of 0.1 mL of 35 wt% DCl/D_2O in 3 mL DMSO. In all cases, the mixtures were sonicated until all solids had completely dissolved.

IRMOF-1,[15,18] IRMOF-3,[15,19] IRMOF-NHPr,[20] IRMOF-NHBu,[20] IRMOF-NHOc[20] and Zn-MOF-74[17] were prepared as previously reported.

2. Synthesis of UiO-66-NHPr, $[Zr_6O_4(OH)_4(bdc\text{-}NHPr)_6]$

The synthesis of UiO-66-NHPr was performed by using an analogous procedure to that of UiO-66-NH_2.[23] In a typical reaction, H_2bdc-NHPr (234 mg, 1.05 mmol) along with $ZrCl_4$ (243 mg, 1.05 mmol) and DMF (12 mL) were loaded into a Teflon lined autoclave. The solution was stirred until the reactants had completely dissolved. The autoclave was placed in an oven and heated at 120 °C for 24 h. The resulting yellow powder was rinsed and centrifuged with MeOH (6000 rpm for 15 min) to remove unreacted H_2bdc-NHPr and residual DMF in the pores. The washing procedure was repeated over 3 days with the solvent replaced every 24 h. Finally, the UiO-66-NH_2 powder was dried under vacuum at 120 °C for 12 h. Figure S1 shows the powder X-ray diffraction pattern for UiO-66-NHPr in comparison to that simulated from the crystal structure of UiO-66, confirming that UiO-66 and UiO-66-NHPr are isostructural.

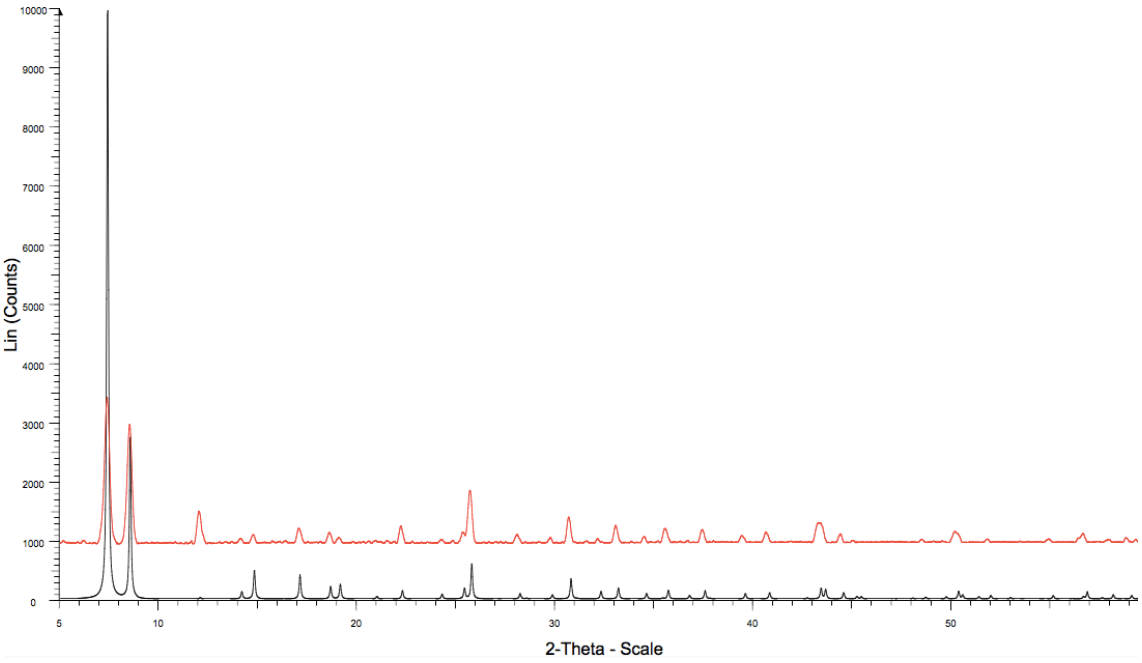

Figure S1. PXRD pattern of UiO-66-NHPr (red) shown together with the simulated PXRD pattern calculated from the UiO-66 crystal structure.[23]

3. Preparation of 3-octanone-loaded IRMOF-NHPr

Method A: Using four equivalents of 3-octanone

IRMOF-NHPr crystals (116 mg, 0.37 mmol) were added in a glass vial containing 5 mL DMF. 3-Octanone (0.23 mL, 1.48 mmol) was then added and the vial was sealed. The mixture was agitated briskly before leaving it to stand at room temperature for 3 days. The crystals were then isolated *via* filtration and rinsed once with fresh DMF (3 mL) to remove any residual 3-octanone on the crystal surfaces. The crystals were rinsed a further once or twice with fresh DMF (3 mL each wash). The NMR spectrum of the sample upon DCl digestion is shown in Figure S2.

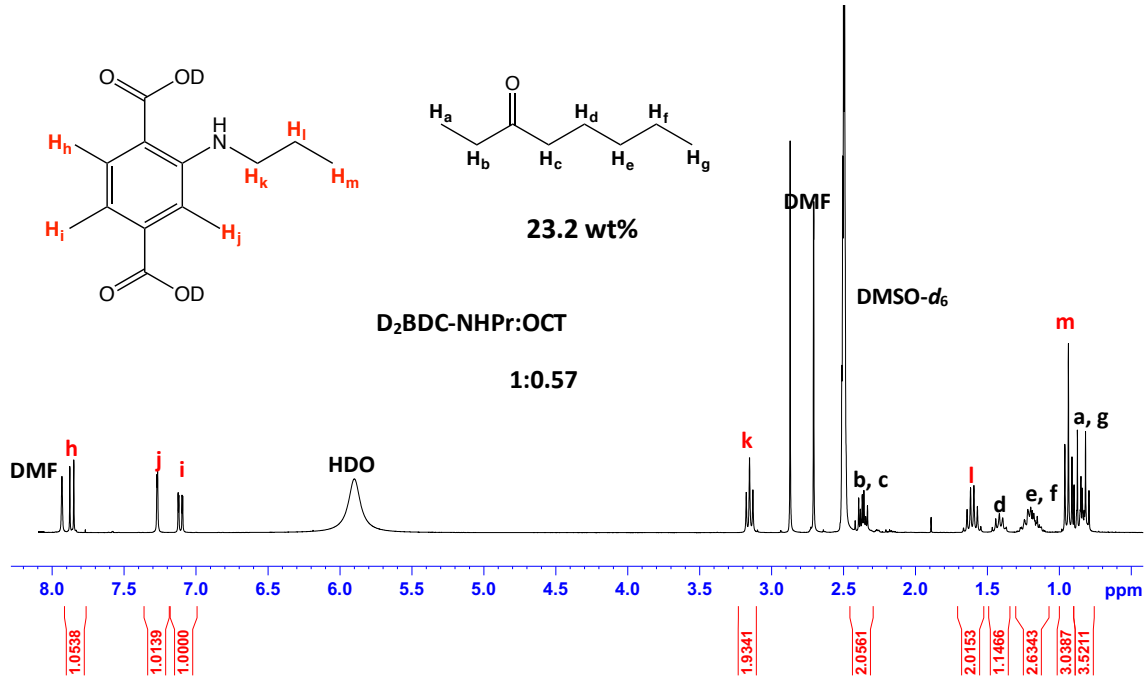

Figure S2. The ^{1}H NMR spectrum for the digested 3-octanone-loaded IRMOF-NHPr.

The 3-octanone loading was determined by comparing the integrals at δ 7.14 ppm and δ 1.45 ppm which correspond to the aryl protons from D_2BDC-NHPr, H_i and alkyl protons, H_d from 3-octanone, respectively. The ratio of D_2bdc-NH_2 to 3-octanone was calculated as being approximately 1:0.57 which gives the chemical formula as $[Zn_4O(bdc\text{-}NHPr)_3]\cdot 1.7oct$ (23.2 wt% 3-octanone loading).

Method B: Using an excess of 3-octanone

IRMOF-NHPr crystals (116 mg, 0.37 mmol) were added in a glass vial containing neat 3-octanone. The vial was sealed and the mixture was agitated briskly before leaving it to stand at room temperature for 3 days. The crystals were then isolated via filtration and rinsed once with

fresh hexane (3 mL) to remove any residual 3-octanone on the crystal surfaces. The crystals were rinsed a further once or twice with fresh hexane (3 mL each wash).

The other MOFs in this study were loaded with 3-octanone or 4-methyl-3-heptanone using analogous procedures. In some cases, MOF samples were activated by chloroform exchange followed by heating under vacuum to remove DMF.

4. Stability studies

Figure S3 shows PXRD patterns for IRMOF-NHPr following activation when left to stand in air. As can be seen from the reduction in peak intensities, crystallinity is lost over the course of 1 h. Figures S4 and S5 show PXRD patterns for IRMOF-NHPr following loading with excess 3-octanone and 4-methyl-3-heptanone, respectively. Loading with either pheromone has been shown to stabilise the MOF with respect to decomposition in air.

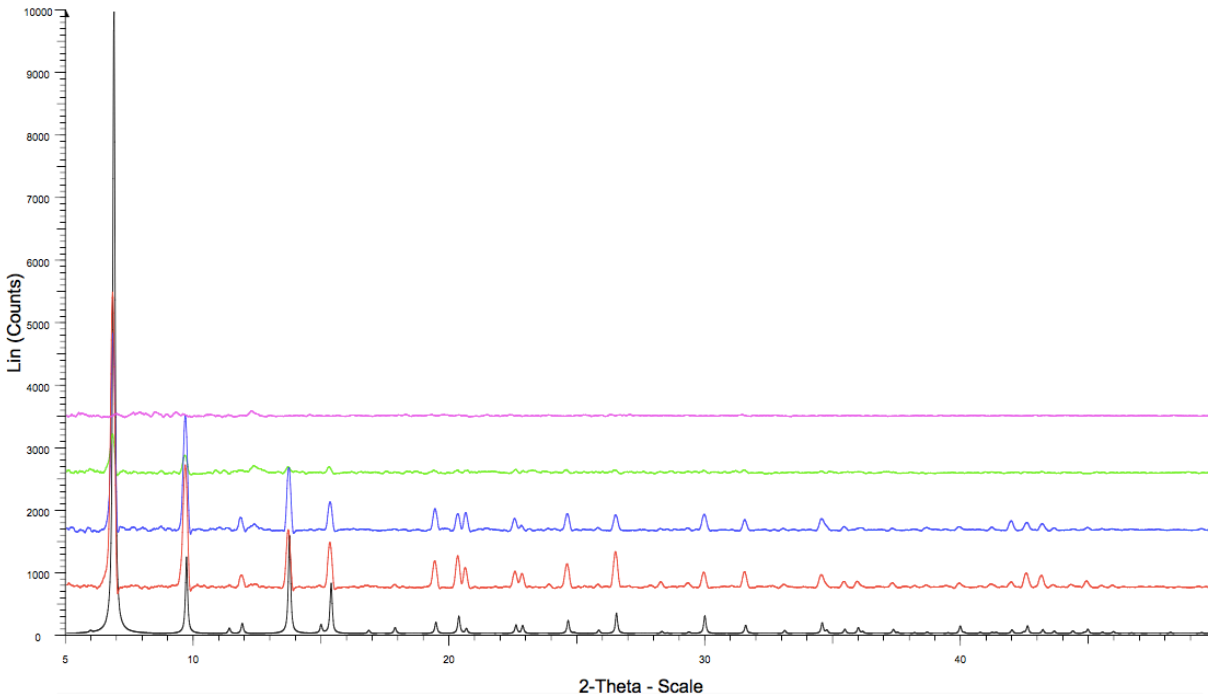

Figure S3. PXRD patterns for IRMOF-NHPr: simulated PXRD pattern from the single crystal X-ray diffraction data for IRMOF-3 (black),[19] PXRD pattern for IRMOF-NHPr upon activation (red), PXRD pattern for activated IRMOF-NHPr after 15 min in air (blue), PXRD pattern for activated IRMOF-NHPr after 30 min in air (green), PXRD pattern for activated IRMOF-NHPr after 1 h in air (pink).

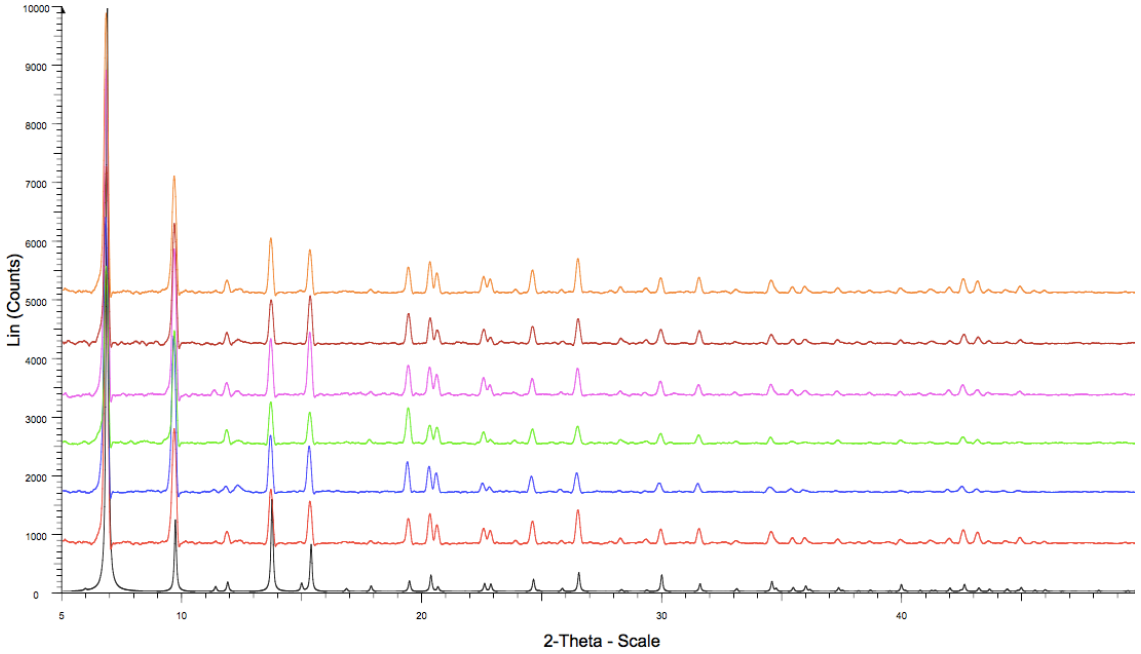

Figure S4. PXRD patterns for IRMOF-NHPr after loading with 3-octanone: simulated PXRD pattern from the single crystal X-ray diffraction data for IRMOF-3 (black),[19] PXRD pattern for IRMOF-NHPr upon activation (red), PXRD pattern for 3-octanone-loaded IRMOF-NHPr after 15 min in air (blue), PXRD pattern for 3-octanone-loaded IRMOF-NHPr after 30 min in air (green), PXRD pattern for 3-octanone-loaded IRMOF-NHPr after 1 h in air (pink), PXRD pattern for 3-octanone-loaded IRMOF-NHPr after 2 days in air (brown), PXRD pattern for 3-octanone-loaded IRMOF-NHPr after 5 days in air (orange).

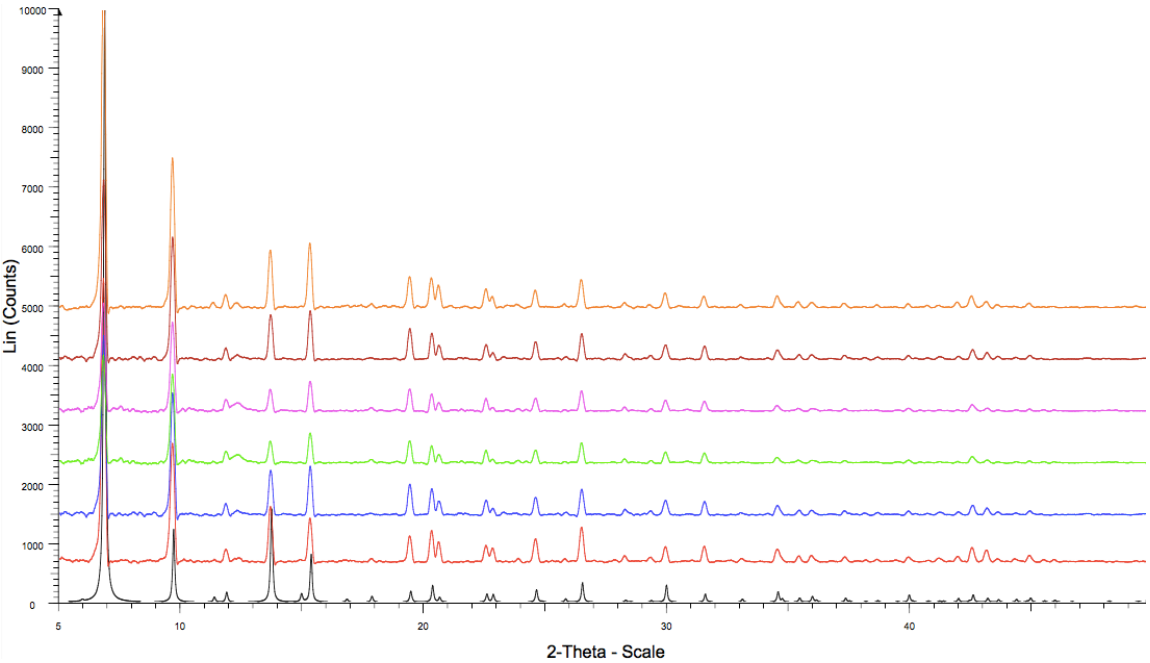

Figure S5. PXRD patterns for IRMOF-NHPr after loading with 4-methyl-3-heptanone (mhp): simulated PXRD pattern from the single crystal X-ray diffraction data for IRMOF-3 (black),[19] PXRD pattern for IRMOF-NHPr upon activation (red), PXRD pattern for mhp-loaded IRMOF-NHPr after 15 min in air (blue), PXRD pattern for mhp-loaded IRMOF-NHPr after 30 min in air (green), PXRD pattern for mhp-loaded IRMOF-NHPr after 1 h in air (pink), PXRD pattern for mhp-loaded IRMOF-NHPr after 2 days in air (brown), PXRD pattern for mhp-loaded IRMOF-NHPr after 5 days in air (orange).

5. Release studies

Pheromone-loaded MOFs were placed in unsealed vials at room temperature and exposed to air. At regular intervals, small samples were taken, digested as described in Section 1 and analysed by ^{1}H NMR spectroscopy, with integrals used to calculate the pheromone remaining in the samples. Each analysis was carried out three times.

Headspace analysis was also undertaken using GC-MS over an eight-day period. The results are summarised in Figure S6, and clearly show evidence for 3-octanone above the solid samples.

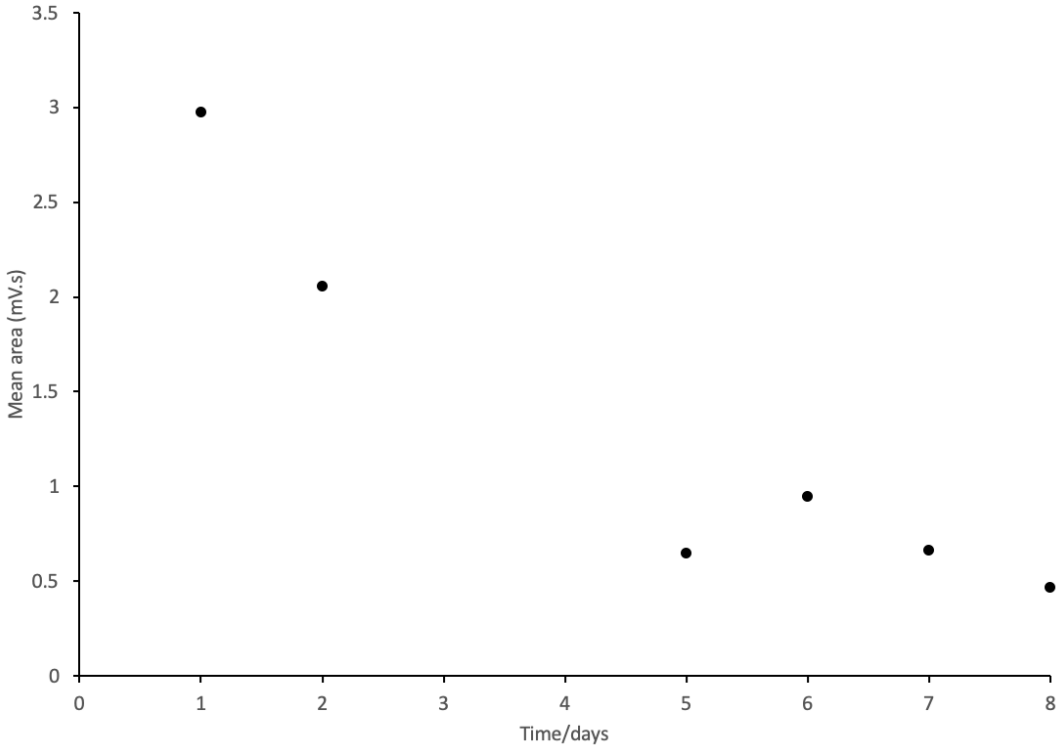

Figure S6. Headspace analysis on a sample of 3-octanone-loaded IRMOF-NHPr, showing the mean area of the 3-octanone peak.

6. Simulation Methods

All simulations were carried out at a loading of 0.156 molecules of 3-octanone molecules / formula unit corresponding to 1.25 molecules / unit cell. To improve statistics, the simulations where carried out in a simulation box comprising 2 × 2 × 2 unit cells. Molecular dynamics simulations were carried out in the NVT ensemble with flexible models for both the frameworks and the 3-octanone molecules using LAMMPS (Large-scale Atomic/Molecular Massively Parallel Simulator).[S1,S2] Cif files of the frameworks were converted to LAMMPS data files using a cif to LAMMPS interface.[S3] The DREIDING force field was employed to describe the framework[S4] and the GAFF force field for the 3-octanone molecules.[S5,S6] The exclusion rules of GAFF and DREIDING are different and in the present work the exclusion

rules of DREIDING were used. Partial charges for the MOFs and the 3-octanone molecules were calculated using the RESP (Restrained Electrostatic Potential) method[S7] implemented in CP2K.[S8,S9] A cut-off radius of 18 Å was used for non-bonded interactions (electrostatics and Lennard-Jones) and tail corrections were applied. Long range electrostatic interactions were computed using the particle-particle-particle-mesh (P^3M) algorithm.[S10] The temperature was maintained at 300 K using the Nose Hoover thermostat.[S11,S12] A time step of 1 fs was employed. After 6 ns of equilibration, data were collected over a production run of 20 ns. Three replicas were run for each simulation.

7. Behavioural Bioassays

The experiments were conducted in a *Eucalyptus* plantation, 20 km from Juiz de Fora, MG, Brazil using thirty small (1-2 foraging entrance holes) *Atta sexdens* colonies. The ant species necessitated use of a mhp-loaded MOF sample as opposed to an oct-loaded sample. A 500 mg sample of $[Zn_4O(bdc\text{-}NHPr)_3]\cdot$mhp was washed with hexane, air-dried to remove traces of DMF and then stored as 50 mg subsamples at –20°C until use. As a positive control, 50 µl of 4-methyl-3-heptanone was applied to a 1 cm diameter rubber disk, left for 5 min to absorb at room temperature, and then stored at –20°C until use. Treatments consisted of 10 g of citrus pulp bait contained sulfluramid insecticide (Mirex-S, Atta-Kill) placed immediately beside the main foraging trail of the colony, 10 cm from the entrance hole. The bait was either applied by itself as a control, or had either a rubber disk with 4-methyl-3-heptanone pheromone (positive control), or a 50 mg sample of $[Zn_4O(bdc\text{-}NHPr)_3]\cdot$mhp placed on top of the bait pile. The numbers of leaf-cutting ant workers approaching to within 2 cm of the bait piles were then counted for 15 min. The numbers of workers counted at the bait piles were compared between the three treatments using a Kruskal-Wallis test in SPSS 25.

8. References

S1. S. Plimpton, *J. Comp. Phys.*, 1995, **117**, 1-19.

S2. https://lammps.sandia.gov/index.html, accessed 21 November 2019

S3. P. G. Boyd, S. M. Moosavi, M. Witman and B. Smit, B. Force-Field Prediction of Materials Properties in Metal-Organic Frameworks, *J. Phys. Chem. Lett.*, 2017, **8**, 357-363.

S4. S. L. Mayo, B. D. Olafson and W. A. Goddard, *J. Phys. Chem.*, 1990, **94**, 8897-8909.

S5. J. Wang, R. M. Wolf, J. W. Caldwell, P. A. Kollman and D. A. Case, *J. Comput. Chem.,* 2004, **25**, 1157-1174.

S6. J. Wang, W. Wang, P. A. Kollman, and D. A. Case, *J. Mol. Graph. Model.,* 2006, **25**, 247-260.

S7. C. I. Bayly, P. Cieplak, W. Cornell and P. A. Kollman, *J. Phys. Chem.*, 1993, **97**, 10269-10280.

S8. J. Hutter, M. Iannuzzi, F. Schiffmann and J. VandeVondele, *Rev. Comput. Mol. Sci.,* 2014, **4**, 15-25.

S9. CP2K: Open Source Molecular Dynamics. http://www.cp2k.org, accessed 21 November 2019

S10. M. Deserno and C. Holm, *J. Chem. Phys.*, 1998, **109**, 7678-7693.

S11. S. S. Nosé, *J. Chem. Phys.*, 1984, **81**, 511-519.

S12. W. G. Hoover, *Phys. Rev. A*, 1985, **31**, 1695-1697.